

# Computer Methods in Biomechanics and Biomedical Engineering

ISSN: 1025-5842 (Print) 1476-8259 (Online) Journal homepage: <http://www.tandfonline.com/loi/gcmb20>

## The twist-to-bend compliance of the Rheum rhabarbarum petiole: integrated computations and experiments

Tanvir R. Faisal, Nicolay Hristozov, Tamara L. Western, Alejandro Rey & Damiano Pasini

**To cite this article:** Tanvir R. Faisal, Nicolay Hristozov, Tamara L. Western, Alejandro Rey & Damiano Pasini (2016): The twist-to-bend compliance of the Rheum rhabarbarum petiole: integrated computations and experiments, Computer Methods in Biomechanics and Biomedical Engineering

**To link to this article:** <http://dx.doi.org/10.1080/10255842.2016.1233328>



Published online: 14 Sep 2016.



Submit your article to this journal [↗](#)



View related articles [↗](#)



View Crossmark data [↗](#)

Full Terms & Conditions of access and use can be found at  
<http://www.tandfonline.com/action/journalInformation?journalCode=gcmb20>

# The twist-to-bend compliance of the *Rheum rhabarbarum* petiole: integrated computations and experiments

Tanvir R. Faisal<sup>a,b</sup>, Nicolay Hristozov<sup>c,d</sup>, Tamara L. Western<sup>c</sup>, Alejandro Rey<sup>e</sup> and Damiano Pasini<sup>a</sup>

<sup>a</sup>Department of Mechanical Engineering, McGill University, Montreal, Canada; <sup>b</sup>Department of Mechanical Engineering, University of Manitoba, Winnipeg, Canada; <sup>c</sup>Department of Biology, McGill University, Montreal, Canada; <sup>d</sup>Department of Cellular and Molecular Medicine, University of Ottawa, Ottawa, Canada; <sup>e</sup>Department of Chemical Engineering, McGill University, Montreal, Canada

## ABSTRACT

Plant petioles can be considered as hierarchical cellular structures, displaying geometric features defined at multiple length scales. Their macroscopic mechanical properties are the cumulative outcome of structural properties attained at each level of the structural hierarchy. This work appraises the compliance of a rhubarb stalk by determining the stalk's bending and torsional stiffness both computationally and experimentally. In our model, the irregular cross-sectional shape of the petiole and the layers of the constituent tissues are considered to evaluate the stiffness properties at the structural level. The arbitrary shape contour of the petiole is generated with reasonable accuracy by the Gielis superformula. The stiffness and architecture of the constituent layered tissues are modeled by using the concept of shape transformers so as to obtain the computational twist-to-bend ratio for the petiole. The rhubarb stalk exhibits a ratio of flexural to torsional stiffness 4.04 (computational) and 3.83 (experimental) in comparison with 1.5 for isotropic, incompressible, circular cylinders, values that demonstrate the relative structural compliance to flexure and torsion.

## ARTICLE HISTORY

Received 25 February 2016  
Accepted 2 September 2016

## KEYWORDS

Flexural stiffness; torsional stiffness; twist-to-bend ratio; rhubarb

## 1. Introduction

Whereas human technology has a long and pragmatic tradition of focusing on rigid structures, nature frequently builds more flexible and adaptable ones. Organisms, especially in the plant kingdom, require stiff structures only in specific circumstances, for instance when a tree must maintain its posture against gravity. Under wind load, however, tree branches can be observed to twist into a more downwind orientation and to cluster together, thus reducing the danger of the tree bending over. A compromise between flexural and torsional stiffness can be observed at a large scale in bamboo culms (Vogel 1995) and banana petioles (Ennos et al. 2000), and at a smaller scale in sedges (Ennos 1993) and daffodil stems (Etnier & Vogel 2000). The flexural and torsional stiffness of a plant organ, such as a stem or petiole, depend on the organ's geometry and the stiffness of its constituent tissues. The ratio of flexural and torsional stiffness, a dimensionless index commonly termed the twist-to-bend ratio, has been widely used to determine the structural compliance of biological beams (Niklas 1992; Vogel 1992, 1995; Etnier & Vogel 2000). The twist-to-bend ratio provides insight

into the factors that influence the relative resistance of a hierarchically structured biological beam to bending vs. twisting.

The petiole, which serves to attach the leaf to the stem, can be considered a hierarchical cellular structure that displays structural features defined at multiple length scales. The hierarchical levels of the rhubarb petiole considered in this work are represented by  $n$ , beginning with the cell wall represented by  $n = 1$  (Figure 1). The structural features below  $n = 1$  are assumed to be amorphous and are not considered in the present study. The material properties of a tissue are largely governed by its heterogeneous cellular microstructure, and this level is represented by  $n = 2$ . The third level of hierarchy depicts the semi-elliptical shape contour of the rhubarb petiole.

Both flexural and torsional stiffness are composite properties that are simultaneously governed by material and geometrical attributes (Wainwright et al. 1982). Therefore a multiscale analysis is required to evaluate the bendiness and twistiness of any biological beam – in this case, a rhubarb petiole. At the first order of hierarchy, the stiffness of parenchymatous and collenchymatous cell

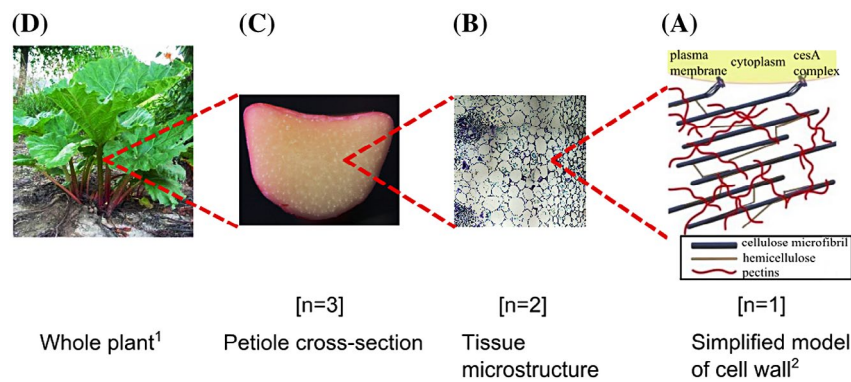


**Figure 1.** Multi-scale hierarchic organization of a plant (*Rheum rhabarbarum*) petiole [<sup>1</sup>Photograph taken by Rosie Lerner, (2000), Purdue University (with permission); <sup>2</sup>Based on Cosgrove (2005)].

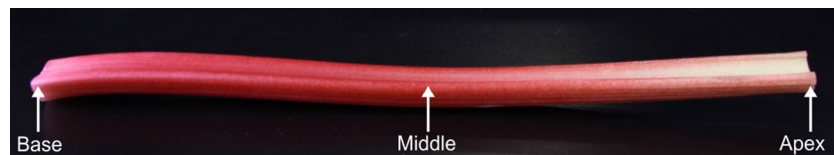


**Figure 2.** A typical rhubarb petiole.

walls can be derived from their chemical composition, the volume fractions, and elastic properties of each major component (Fratzl et al. 2004; Kha et al. 2008; Faisal et al. 2013). The mechanical properties of the cell walls are then used to compute the effective stiffness of the surrogated model of each constituent tissue using for example the Finite-edge Centroidal Voronoi Tessellation method at the second hierarchical order (Faisal et al. 2012, 2014). The contribution of the constituent tissues' microarchitecture is thereby incorporated in evaluating the overall mechanical behavior of the petiole.

The overall morphology of a petiole (biological beam) plays an important role in determining its flexural and torsional rigidity. Petioles with an apical groove tend to display higher twist-to-bend ratios than petioles with a circular cross-section (Vogel 1992, 1995). The effect of the cross-sectional geometry of the petiole can be theoretically modeled with schemes based on shape factors (Ashby 2005) and shape transformers (Pasini 2008b). Although shape factors depend on both the size and shape of a cross-section, shape transformers allows to decouple the shape and size, and gain further insight into the role of cross-section geometry on the mechanical properties of a structure. In this work, we investigate the influence of the petiole's cross-sectional shape and multi-tissue layered architecture to its flexural and torsional rigidity via the shape transformers scheme. To this extent, the cross-sectional shape, which varies along the length of this tapered petiole, is described through the Gielis parameterization of the Lamé curves (Gielis 2003).

This work is intended to examine the bendiness and twistiness of hierarchically structured rhubarb petiole to characterize its compliance attributes. The irregular cross-sectional shape of the petiole and the layers of the constituent tissues are considered in modeling its stiffness properties. The hierarchically derived material properties and the generated irregular shape contour have been used here to computationally determine the petiole's twist-to-bend ratio with reasonable accuracy, as compared with experimental data. The reported work can offer inspiration for biomimetic structural design since it helps to provide insights into the structural efficiency of biological beams.

## 2. Materials and methods

Fresh rhubarb petioles were obtained from produce suppliers 'The Greenery' (Barendrecht, Netherlands) and 'Dragonberry Produce' (Clackamas, OR, U.S.A). They were stored at 4 °C in plastic bags to prevent decay and dehydration. A typical rhubarb petiole with different sections is shown in Figure 2. Roughly uniform along its length, the petiole tapers slightly from base to apex and displays a subtle change in cross-sectional shape.

### 2.1. Model plant

*Rheum rhabarbarum*, popularly known as rhubarb, is a hardy, perennial, dicotyledonous plant that grows from a bulbous rhizome, forms thick and long leaf stalks

**Table 1.** Example of typical parameters used to plot the shape contours of the cross-sectional shape of rhubarb petiole.

| Lengthwise petiole location | $m$ | $n_1$ | $n_2$ | $n_3$ | $a$  | $b$ |
|-----------------------------|-----|-------|-------|-------|------|-----|
| Basal                       | 8   | 2.9   | 3.1   | 2.9   | 0.76 | 1.1 |
| Middle                      | 7.7 | 2.8   | 4.1   | 2.3   | 0.76 | 1.1 |
| Apical                      | 7.8 | 2.5   | 3.0   | 3.5   | 0.9  | 1.3 |

(petioles) that bear large, heart-shaped leaves of up to 1 m<sup>2</sup> in size (Figure 1(D)). The cross-section of the rhubarb petiole is roughly semi-elliptical with an adaxial groove (Schrader 2008; Pasini 2008b; Huber et al. 2009). The typical size of the rhubarb plant varies from 0.9 to 1.5 meters in height and 0.9–1.2 meters in diameter. The fleshy petiole is slender with a length of up to 72 cm and 2.5–5.0 cm in diameter (Schrader 2008; Huber et al. 2009). However, the width (diameter) of the investigated rhubarb petioles ranged between 1.4 and 3.1 cm, whereas the length varied between 35 and 55 cm.

In cross-section, the rhubarb petiole has three major structural components (moving from outside to inside): epidermis, collenchyma and parenchyma. The majority of the cross-sectional area (~90%) is occupied by a relatively soft core composed mainly of large, thin-walled parenchyma cells with small air spaces between them. Vascular bundles are embedded diffusely throughout the core tissue and appear to play a role in stiffening and strengthening the petiole (Huber et al., 2009). The core is surrounded by collenchyma cells arranged in several layers. These cells are much smaller than typical parenchyma cells and also lack secondary cell walls. The collenchyma tissue is surrounded by a very thin epidermal monolayer, which in turn is covered by a waxy cuticle that insulates the petiole from water loss.

## 2.2. Computational modelling approach

### 2.2.1. Irregular cross-section and its geometric properties

The shapes of biological structures are often asymmetric and display complex forms as adaptations to their ecological context. Since geometry affects the overall mechanics of an organ, these shapes and their geometric properties need to be modelled accurately, although natural shapes are usually difficult to represent. In this work, the irregular cross-sectional shapes are generated using Gielis parametrization of the Lamé curves [need ref here], mimicking the natural form of the petioles. The arbitrary shape contour of the rhubarb stalk is generated by the Gielis curve in polar coordinates by the function  $r(\phi)$  as follows:

$$r = f(\phi) = \frac{1}{\sqrt[n_1]{\left(\left|\frac{1}{a} \cos\left(\frac{4}{m}\phi\right)\right|\right)^{n_2} + \left(\left|\frac{1}{b} \sin\left(\frac{4}{m}\phi\right)\right|\right)^{n_3}}} \quad (1)$$

where  $n_i \in \mathbb{R}^+$  and  $a, b, m \in \mathbb{R}_*^+$ ; parameters  $a$  and  $b$  control the scale,  $4/m$  represents the number of rotational symmetries, and  $n_1, n_2$ , and  $n_3$  are the shape coefficients.  $m$  is a positive integer, when the curve is closed and not self-intersecting.

To determine the values of the parameters in Equation (1), the trace of the petiole's cross-sectional shape was drawn within the smallest possible rectangle that can inscribe it. The parameters  $a$  and  $b$  were the half of the length and width of the rectangle, respectively. The values of other parameters,  $m, n_1, n_2$ , and  $n_3$  were determined by trial values and non-linear search algorithms. Typical parametric values for the petiole's cross-sectional shape contours at different sections (Figure 2) are shown in Table 1, and the respective shape contours have been modelled based on these using Equation (1).

The actual cross-sectional shapes of the rhubarb petiole at basal, mid, and apical sections, and their corresponding surrogated shape contours are shown in Figure 3. In the computational analysis carried out in this work, the mid-basal and mid-apical sections are not considered because of their close resemblance to the basal and apical sections, respectively.

The geometric properties, such as area ( $A$ ) and second moment of area ( $I$ ), are computed numerically by discretising the irregular shape contour, where closed form expressions are unable to calculate the geometric quantities. Using Green's theorem, the domain integral is transformed into a line integral, which is computed with quadratic elements that represent the coordinates over the curve. The procedure yields exact formulae for the shapes enclosed by boundaries that can be represented by 1<sup>st</sup> or 2<sup>nd</sup> order polynomials. The second moment of area is calculated for two orthogonal axes of the cross-sectional shape.

### 2.2.2. Flexural and torsional stiffness of surrogated rhubarb cross-section

The shape transformers method (Pasini et al. 2003, 2006; Pasini 2006, 2007) is used first to bridge the two levels of the hierarchy from  $n = 1$  (cell wall) to  $n = 2$  (cellular tissues) of rhubarb stalk; then it is used together with the Gielis parametrization of the shape petiole contour to obtain the geometric properties,  $I$  and  $J_T$  (torsional constant) of the petiole's cross-section at the third hierarchical level. With this method, a geometric quantity of the petiole's cross-section is normalized by the same geometric quantity of the surrounding rectangular envelope,  $D$ . The shape of the cross-section enclosed in  $D$  is represented by the dimensionless property  $S$  (Figure 4). The dimensionless shape transformer,  $\psi_g$ , of the geometric quantities,  $g$ , of the cross-section is defined by:

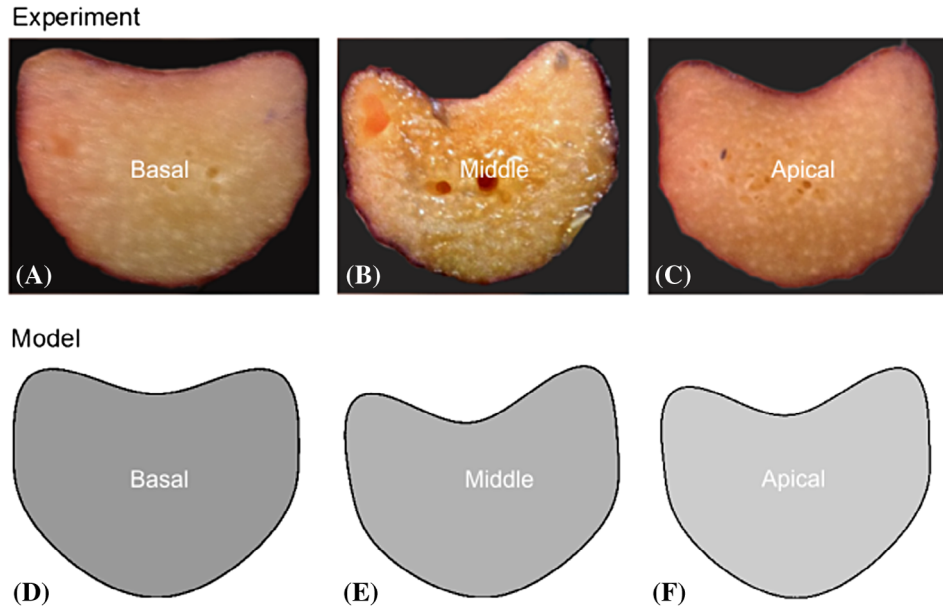


**Figure 3.** Cross-sectional images of basal, middle, and apical sections of rhubarb petiole (A)–(C) [top row] and their corresponding surrogated shape contours (D)–(F) [bottom row].

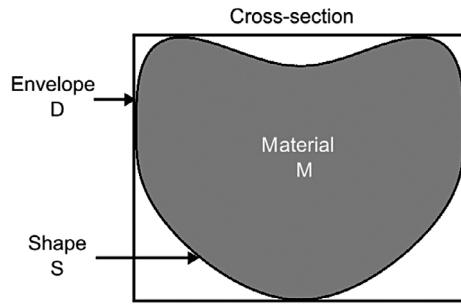


**Figure 4.** The components of the shape transformers method showing shape (S) and envelope (D) for the rhubarb cross-section.

$$\psi_g = \frac{g}{g_D} \quad (2)$$

where  $g_D$  is any geometric quantity of the envelope. The scheme of shape transformers,  $\psi_g$ , can be applied to calculate the bending and torsional stiffness of the shape contour of rhubarb cross-sections, where the respective shape transformers can be expressed as  $\psi_A = \frac{A}{A_D}$ ,  $\psi_I = \frac{I}{I_D}$  and  $\psi_J = \frac{J}{J_D}$ , with the denominators representing the geometric quantities of the envelope and the numerators describing the geometric quantities of the petiole's cross-section (Pasini & Mirjalili 2006; Pasini 2007, 2008a).

An idealized example is presented in Figure 5(a) to illustrate the effect of material structuring and how this process can be modelled with shape transformers (Figure 5(A)). Four levels of hierarchy have been displayed in the cross section, where the elements are assumed to be continuous at each level. The material  $M_0$  is considered to be uniform and shapeless at order 0.  $M_0$  becomes a solid

circular two-dimensional structure when shaped. During this process,  $M_0$  is transformed to the shaped material  $M_1$  at level  $n = 1$ , where  $M_1$  inherits properties  $M_0 g_1$ . Hence, the effective flexural property  $E_1$  at the first level of the hierarchy is obtained by normalizing  $E_0 I_1$  with the envelope property  $I_{D_1}$  and is expressed as:

$$E_1 = E_0 \frac{I_1}{I_{D_1}} = E_0 \psi_I^1 \quad (3)$$

where  $\psi_I$  is the shape transformers for the second moment of area. A similar scheme is followed for the rhubarb petiole, assuming that the first level exhibits isotropic and uniform material properties. The flexural stiffness at the second level of hierarchy (tissue level) can be expressed as:

$$E_2 = E_1 \psi_I^2 = E_0 \psi_I^1 \psi_I^2 \quad (4)$$

Hence, the effective Young's modulus at the  $n^{\text{th}}$  order can be expressed as a ratio of effective material properties:

$$\frac{E_n}{E_0} = \prod_{j=1}^n \psi_I^j \quad (5)$$

where  $n = 2$  has been considered in the present analysis. To factor in the overall structure size,  $E_n$  in Equation (5) can be rearranged and used to evaluate the flexural and torsional rigidity of the rhubarb stalk considered in this work.

For the layered architecture of the petiole, the geometry of each layer can be expressed in terms of the shape transformers,  $\psi_{A_i}$  for area,  $\psi_{I_i}$  for moment of area and  $\psi_{J_i}$  for

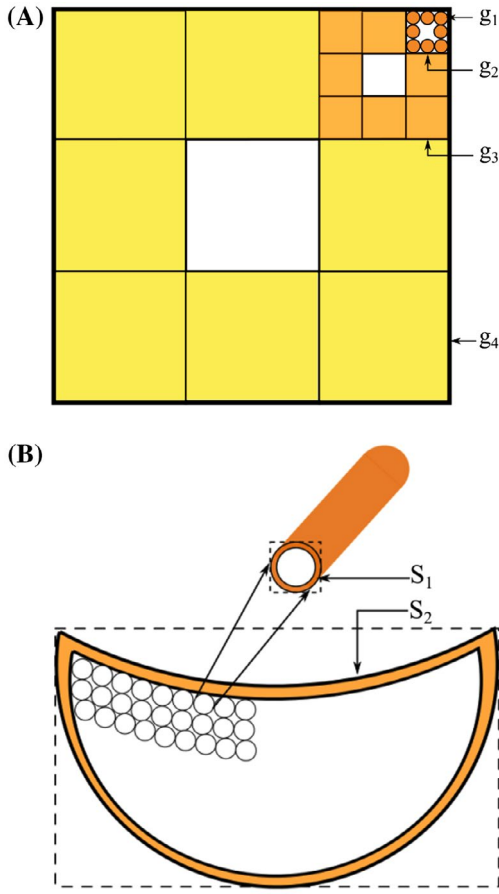


**Figure 5.** (A) An ideal cross-section structure. (B) Structural hierarchies of a petiole [adapted from Pasini (2008a)].

polar moment of area. Hence, the effective properties of a multi-layered petiole consisting of different geometrical, material, and mechanical properties at each layer can be shown as:

$$E_D = \sum_{i=1}^k E_i \frac{I_i}{I_D} = \sum_{i=1}^k E_i \frac{\int_{A_i} y_i^2 dA}{I_D} = \sum_{i=1}^k E_i \psi_{I_i} \quad (6a)$$

$$\rho_D = \sum_{i=1}^k \rho_i \frac{A_i}{A_D} = \sum_{i=1}^k \rho_i \psi_{A_i} \quad (6b)$$

where  $k = 2$  for the current approach. Coupled with the cross-sectional shape of each layer of tissue, the transformed flexural modulus and density for the  $k^{\text{th}}$  layer can be expressed as:

$$E_{T_{\text{layer}}} = \psi_I E_D = \underbrace{\psi_I}_s \sum_{i=1}^k E_i \psi_{I_i} \quad (7a)$$

$$\rho_{T_{\text{layer}}} = \psi_A \rho_D = \underbrace{\psi_A}_s \sum_{i=1}^k \rho_i \psi_{A_i} \quad (7b)$$

For a layer of cellular tissue, the contribution of cellular structuring can be factored in by replacing  $E_i$  in Equation (5) with  $E_{T_i}$  in Equation (7a) and expressed as:

$$E_T = \sum_{i=1}^k \left( E_0 \prod_{j=1}^n \psi_I^j \right) \psi_{I_i} \quad (8)$$

This rationale can also be used to evaluate the torsional stiffness of the petiole and expressed as:

$$J_T = \sum_{i=1}^k \left( J_0 \prod_{j=1}^n \psi_J^j \right) \psi_{J_i} \quad (9)$$

where  $J_T$  is the torsional constant of the cross-sectional shape. The preceding rationales are typically used to evaluate the compliance of a petiole, under wind and gravity loads. Therefore, the ratio of bendiness to twistiness (which is typically known as the *twist to bend* ratio) of the rhubarb petiole can be written as:

$$\frac{EI}{GJ_t} = \frac{\sum_{i=1}^k \left( E_0 \prod_{j=1}^n \psi_I^j \right) \psi_{I_i} I_{Dn}}{\sum_{i=1}^k \left( G_0 \prod_{j=1}^n \psi_J^j \right) \psi_{J_i} J_{Dn}} \quad (10)$$

where  $G$  is the shear modulus,  $n = 2$  and  $k = 2$ . This ratio represents the compliance of the surrogate petiole. We recall here that the method of shape transformers is an alternative method of homogenization that allows gaining insight into the mechanical properties of hierarchical structures. It can capture concurrently the effect of cross-section shape, multi-layered tissues, and cellular structuring in a cellular component. Whereas in classical homogenization methods the effective material properties are calculated from the volume fraction of the inclusion, with the scheme adopted in this work the elastic properties of each constituent can be modelled at each level of the structural hierarchy, thereby providing a direct insight into the relationship between effective stiffness and microstructural geometry.

### 2.3. Flexural and torsional tests for large petioles

An apparatus was built in-house to perform three point-bending tests of large petioles. This was essentially a large universal testing machine with a conventional upright design in which a linear potentiometer (Omega, Laval, QC, Canada) measured crosshead displacement,

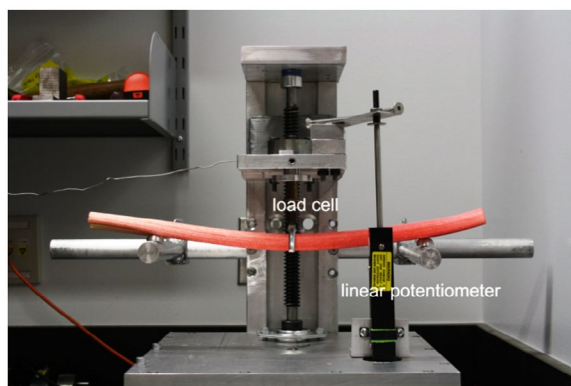


**Figure 6.** Three-point bending test of a rhubarb petiole using an apparatus built in-house.

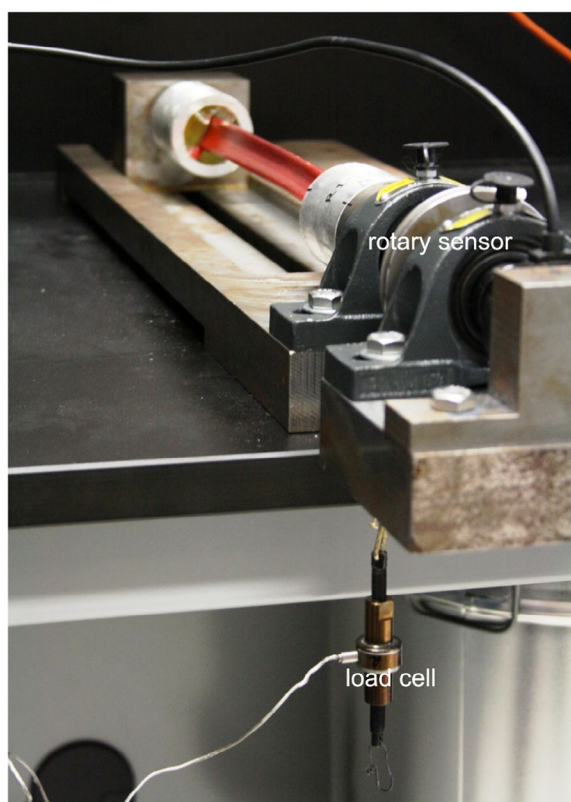


**Figure 7.** Torsion test of a rhubarb petiole.

and a 10 lb load cell (Honeywell, Columbus, OH, U.S.A) measured force. The crosshead was actuated via a hand-operated crank connected to a vertical worm gear and was designed to apply force to the center of a sample supported by two crossbeams. This apparatus was used to test the flexural stiffness of 15 petiole samples. Samples, groove side down, were placed on aluminium supports with a span length of 287 mm, and force was applied to the sample centre through a semi-annular probe (Figure 6). After testing, the cross-sectional geometry of each petiole was sampled at five equally spaced points along its length.

Section height and width were measured using digital calipers, and hand-cut sections were imaged using a digital camera. The outline of each section was drawn and scaled by a design graphics software package (AutoCAD, Autodesk Inc.), which allowed us to calculate the geometric properties  $A$ ,  $I_{xx}$ , and  $I_{yy}$ .

An apparatus was also built for testing torsional rigidity (Figure 7). A separate set of 15 petioles were subjected to torsion testing. Samples measured between 270 and 310 mm in length. Each end was fixed inside an aluminium cylinder using cyanoacrylate glue (Loctite® 416, Henkel) and epoxy resin (Scotch-Weld®, 3 M). One cylinder was fixed in position while the other was attached to a pulley. The pulley was rotated by applying force through a hand crank connected to a load cell, which was used for calculating torque. Variable torque was applied while keeping the speed of rotation constant, and sample deformation was calculated by measuring the angle of deflection on that pulley using an attached rotary sensor. After testing, each petiole was similarly sampled for cross-sectional geometry and the geometric properties,  $A$ ,  $I_{xx}$ , and  $I_{yy}$  were determined, and torsional constant,  $J_T$ , were determined from  $I_{xx}$  and  $I_{yy}$  to determine the torsional stiffness of the petiole.

For both devices, real-time load, position, and angle data was recorded using an ADMET MTEST Quattro hardware (ADMET, Inc., Norwood, MA) unit with accompanying software. In both tests, a consistent cross-head speed was maintained by monitoring a time-position or time-angle plot as each sample was loaded as shown in Figure 8(A) and (B). Each sample was subjected to three cycles of loading and unloading to assess its elastic and plastic deformation behavior.

#### 2.4. Tissue density

The mass of whole rhubarb petioles and isolated tissue samples was measured using a laboratory scale. The volume of whole petioles was estimated by measuring their water displacement inside a 1000 or 2000 mL graduated cylinder. The volume of isolated tissue samples was calculated from geometric measurements taken manually with digital calipers.

### 3. Results and discussion

#### 3.1. Cross-sectional geometry and tissue density

Each petiole was sampled at five equally spaced points by making hand-cut sections immediately after testing. The distribution of cross-sectional area and geometrical properties is shown in Appendix 1 (Figures A1–A4). The box and whisker plots depict the distribution of area

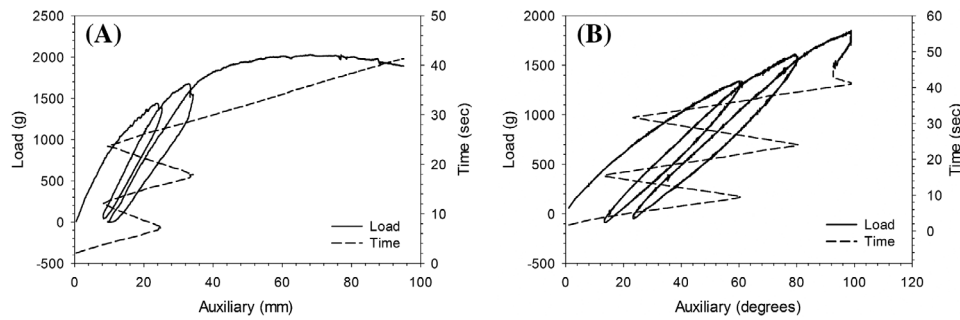


**Figure 8.** Cyclic flexural and torsional tests of the rhubarb petiole. (A) Typical load-position plot from bending test, where dotted line represents time vs. position. (B) Typical load-angle plot from torsion test, where dotted line represents time vs. angle.

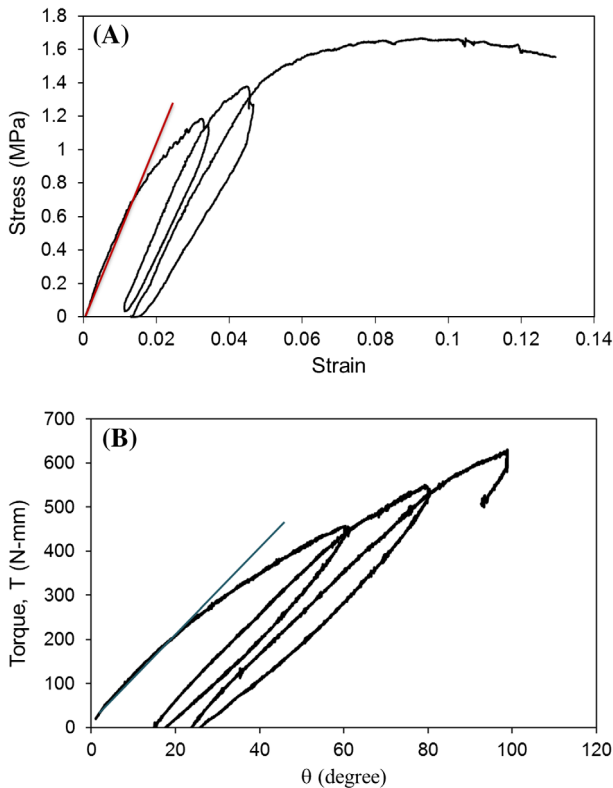


**Figure 9.** (A) Stress-strain plot of a rhubarb petiole subjected to cyclic flexural testing. (B) Torque-angle of twist plot of a rhubarb petiole subjected to cyclic torsion testing.

and  $I_{xx}$  of all the petioles that underwent flexural testing (see Appendix 1 in Figures A1 and A2), and the area and  $J_T$  of the rhubarb petioles used for torsional testing (see Appendix 1 in Figures A3 and A4), respectively. A gradual decrease in cross-sectional area was observed, amounting to 19.1 and 16.6% mean reduction from base to apex of each set of 15 samples for flexural and torsion tests, respectively. A reduction of 31.96 and 28.27% was also observed in  $I_{xx}$  and  $J_T$ , respectively. The reduction in all four values is statistically significant when comparing basal and apical sections. Additionally, the cross-section gradually changed from a D to C shape, as the adaxial

groove became deeper near the apex (see Appendix 1 in Figure A5). Isolated core tissue also displayed a density reduction of 13.6% from base to apex, dropping from  $0.939 \text{ g/cm}^3$  ( $\pm 0.005 \text{ S.E.}$ ) to  $0.881 \text{ g/cm}^3$  ( $\pm 0.005 \text{ S.E.}$ ). Whole petioles displayed a mean density of  $0.915 \text{ g/cm}^3$  ( $\pm 0.013 \text{ S.E.}$ ), suggesting a major contribution from basal core tissue to their overall properties.

### 3.2. Flexural and torsional rigidity of the rhubarb petiole

In both torsion and bending tests, samples smoothly transitioned from an initial linear-elastic behavior into plastic deformation. Elastic moduli were calculated from the linear-elastic region of the load-position and load-angle curves as shown in Figure 9 using the corresponding geometric properties of the cross-sectional shapes determined from the CAD models. These experiments yield a mean elastic modulus, ( $E$ ), of 30.8 MPa and a mean shear modulus, ( $G$ ), of 2.74 MPa. The mean flexural rigidity,  $EI$ , and torsional rigidity,  $GJ_T$ , have been determined to be  $0.224 \text{ N} \cdot \text{m}^2$  ( $\pm 0.03 \text{ S.E.}$ ) and  $0.0586 \text{ N} \cdot \text{m}^2$  ( $\pm 0.009 \text{ S.E.}$ ), respectively; and yield an  $EI/GJ_T$  ratio of  $3.83(\pm 1.11 \text{ SD})$ . This experimental ratio corresponds well with the  $EI/GJ_T$  predicted by the computational model developed using the shape transformers method, that ratio being  $4.04(\pm 0.65 \text{ SD})$  – averaged across basal, middle and apical regions of the stem. Figure 10 shows a comparison of experimental  $EI/GJ_T$  of rhubarb petioles and the computational twist-to-bend ratio of petiole's surrogated cross-sectional shape contours at each of the three distinct locations. The experimentally determined  $EI/GJ_T$  for intact petioles is most similar to that predicted for the apical cross-section.

### 3.3. Twist-to-bend ratio of rhubarb petiole and its compliance

The mean experimental  $EI/GJ_T$  of rhubarb petioles matches reasonably well with the computed ratio. The



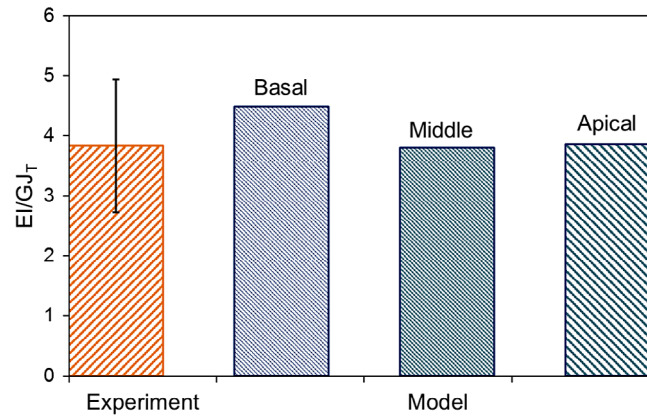


**Figure 10.** Comparison of experimental and computational twist-to-bend ratio.

computational result is derived from the correlation of surrogated cross-sectional geometry, tissue distribution, and structural properties of rhubarb tissue. The correspondence between model and experiment suggests that these three are the primary factors underlying the twist-to-bend anisotropy of the rhubarb petiole. Smaller-scale structural features such as cell wall and tissue anisotropy also likely play roles, as would the continuous taper and changes in properties along the petioles, but their contributions appear to be relatively minor.

The actual twist-to-bend ratio of rhubarb of 3.83 ( $\pm 1.11$  SE) is moderate and approaches that of the similarly-shaped, though smaller, petioles of sweetgum  $EI/GJ_T$  of 5.1 ( $\pm 1.3$  SD) and green bean  $EI/GJ_T$  of 4.9 ( $\pm 2.1$  SD) (Vogel 1992). This is in contrast to the *U*-shaped banana (*Musa textilis*) petiole, which has an  $EI/GJ_T$  of 40–100. This extreme ratio in banana is likely due to the internal structure of its petioles, which have a central core with large air spaces (aerenchyma) and consequently peripheral localization of reinforcing elements (Ennos et al. 2000). Conversely, rhubarb petioles are mostly composed of a solid parenchymous core with diffuse distribution of vascular bundles as usual for monocots (Huber et al. 2009). This tissue organization, combined with other structural properties, is likely responsible for the moderate degree of twist to bend anisotropy for rhubarb petioles despite their grooved shape.

The material properties  $E$  and  $G$  are the cumulative outcome of the preceding levels of the hierarchy,  $n = 1$  (cell wall) and 2 (tissue microstructure), whereas the geometric properties,  $I$  and  $J_T$ , represent the contribution of the topmost level (petiole cross-section). Without considering material properties, the twist-to-bend ratio ( $I/J_T$ ) of rhubarb petiole is 1.05–1.60 (Pasini 2008b). The contribution of material anisotropy increases the twist-to-bend ratio considerably and reflects the influence of the multiple orders of the structural hierarchy. To develop a comprehensive model that also accounts for

the heterogeneity of the base material, the anisotropy of the cell wall material should be integrated in the multi-scale model. The mechanical anisotropy of the plant cell wall is mainly governed dictated by the orientation of the cellulose microfibrils, which in turns depends on the cell-type, cell maturity and environmental context. However, it is technically challenging and outside the scope of this article to mechanically test isolated cell wall material and to measure the microfibril angle. In addition, the current computational model still does not account for all of the tissue types present in the rhubarb petiole. The tissues (e.g. epidermal layer and vascular bundles) that have been neglected, despite constituting only a small fraction of the petiole's volume, might affect the mechanical properties of the petiole in unpredicted ways. It is also assumed that perfect bonding exists between the two layers, the parenchyma and surrounding collenchyma, represented in the model, which may not be entirely realistic. Moreover, the errors due to the above assumptions could propagate from lower to higher hierarchical level, and consequently accumulate at the topmost level of the hierarchy. Despite the simplification in modelling and the limitations in obtaining experimental data at each hierarchical level, the small difference between experimental and computational twist to bend ratios validates the accuracy of the modelling approach presented in this work. Moreover, from a mechanistic point of view, both shape and material properties influence  $EI/GJ_T$ , as it 1.5 for a cylinder of an isovolumetric material. The deviation of the  $EI/GJ_T$  ratio for rhubarb petioles from that for a circular cross-section indicates the ease of twisting relative to bending. The grooved non-circular shape reduces the torsional rigidity to a greater extent than a circular cross-section and ultimately affects the twist to bend ratio of the overall rhubarb stalk. While petioles must often twist easily, allowing leaves to cluster together and reduce their drag under wind loads, they must not bend too easily because they function as cantilevers that

must support the leaf. Plants can achieve high values of  $EI/GJ_T$  through the gradual adjustment of material and geometry, and the ratio also varies along the structure. This variation is also reflected in the computational model, where  $EI/GJ_T$  at the base is 16.3% higher than at the apex. Hence, the twist-to-bend ratio can be used to assess the structural efficiency of a cross-sectional shape in minimizing wind drag while preventing sagging under heavy load.

#### 4. Conclusion

The study of biological structures is essential to the development of novel biomimetic technologies. This work presents a step forward in understanding how plants exploit structural and functional integration at each level of the structural hierarchy. The development of bio-inspired compliant materials and structures based on the natural principles of self-assembly, anisotropy, cellularity, and irregular morphology requires an investigative approach that bridges biology and engineering modelling. In this work, we have examined the flexural and torsional stiffness of the rhubarb stalk. To replicate the overall stiffness computationally, the stiffness properties of the preceding hierarchies have been included. The effect of cross-sectional shape in determining flexural and torsional rigidity has also been confirmed. With respect to tissue properties, the cross-sectional shape plays a substantial role in determining the compliance of the petiole. The characteristic grooved non-circular cross-section facilitates the twisting of the petiole without lowering the flexural stiffness. The experimental results characterize the compliance behavior of the actual petiole, whereas the computational model demonstrates the feasibility of using multiscale modelling to capture mathematically the compliance of a petiole. This may provide insight into the structural efficiency of a rhubarb petiole and may also help to guide the design of future bio-inspired structures.

#### Acknowledgments

The authors would like to thank Lucy Federico of the Department of Biology, McGill University for providing micrographs of rhubarb tissue.

#### Disclosure statement

No potential conflict of interest was reported by the authors.

#### Funding

This research is supported by a grant from the Fonds de Recherche du Québec–Nature et Technologies (FQRNT).

#### References

- Ashby MF. 2005. Materials selection in mechanical design. 3rd ed. Oxford: Elsevier Butterworth-Heinemann.
- Cosgrove DJ. 2005. Growth of the plant cell wall. *Nat Rev Mol Cell Biol.* Nov;6:850–861.
- Ennos AR. 1993. The mechanics of the flower stem of the sedge *Carex acutiformis*. *Ann Bot.* Aug 1;72:123–127.
- Ennos AR, Spatz HC, Speck T. 2000. The functional morphology of the petioles of the banana, *Musa textilis*. *J Exp Bot.* Dec 1;51:2085–2093.
- Etnier SA, Vogel S. 2000. Reorientation of daffodil (*Narcissus: Amaryllidaceae*) flowers inwind: drag reduction and torsional flexibility. *Am J Bot.* Jan 1;87:29–32.
- Faisal T, Rey A, Pasini D. 2013. A multiscale mechanical model for plant tissue stiffness. *Polymers.* 5:730–750.
- Faisal TR, Hristozov N, Rey AD, Western TL, Pasini D. 2012. Experimental determination of *Philodendron melinonii* and *Arabidopsis thaliana* tissue microstructure and geometric modeling via finite-edge centroidal Voronoi tessellation. *Phys Rev E.* 86:031921.
- Faisal TR, Hristozov N, Western TL, Rey AD, Pasini D. 2014. Computational study of the elastic properties of *Rheum rhabarbarum* tissues via surrogate models of tissue geometry. *J Struct Biol.* 185:285–294.
- Fratzl P, Burgert I, Gupta HS. 2004. On the role of interface polymers for the mechanics of natural polymeric composites. *Phys Chem Chem Phys.* 6:5575–5579.
- Gielis J. 2003. A generic geometric transformation that unifies a wide range of natural and abstract shapes. *Am J Bot.* Mar;90:333–338.
- Huber T, Graupner N, Müssig J. 2009. As tough as it is delicious? A mechanical and structural analysis of red rhubarb (*Rheum rhabarbarum*). *J Mater Sci.* 44:4195–4199.
- Kha H, Tumble S, Kalyanasundaram S, Williamson RE. 2008. Finite element analysis of plant cell wall materials. In: Bell J, Yan C, Ye L, Zhang L, editors. *Frontiers in materials science and technology*. Stafa-Zurich: Trans Tech Publications Ltd; p. 197–201.
- Lerner R. 2000. It's Rhubarb Time! [Internet]. Purdue (IN): Purdue Yard & Garden News. Available from: <https://agriculture.purdue.edu>
- Niklas KJ. 1992. *Plant biomechanics*. Chicago, IL: The University of Chicago Press.
- Pasini D. 2006. Shape and material selection for optimizing flexural vibrations in multilayered resonators. *J Microelectromech Syst.* 15:1745–1758.
- Pasini D. 2007. Shape transformers for material and shape selection of lightweight beams. *Mater Des.* 28:2071–2079.
- Pasini D. 2008a. Modelling the micro- and macro-structure efficiencies of a compliant petiole beam. In: Brebbia CA, editor. *Design and nature IV: comparing design in nature with science and engineering*. Southampton: WIT Press; p. 107–117.
- Pasini D. 2008b. On the biological shape of the Polygonaceae *Rheum rhabarbarum* petiole. *J Des Nat Ecodyn.* 3:1–26.
- Pasini D, Burgess S, Smith D. 2006. A method for selecting macro-scale structures with axially loaded members. *Int J Mech Mater Des.* Jun 1;3:185–199.
- Pasini D, Mirjalili V. 2006. The optimized shape of a leaf petiole. In: Brebbia CA, editor. *Design and nature III: comparing design in nature with science and engineering*. Southampton: WIT Press; p. 35–45.

Pasini D, Smith DJ, Burgess SC. 2003. Structural efficiency maps for beams subjected to bending. *Proc Inst Mech Eng Pt L-J Mater-Des Appl.* 217:207–220.

Schrader WL. 2008. Rhubarb production in California. *Journal.* Available from: <http://anrcatalog.ucdavis.edu/>

Vogel S. 1992. Twist-to-bend ratios and cross-sectional shapes of petioles and stems. *J Exp Bot.* Nov 1;43:1527–1532.

Vogel S. 1995. Twist-to-bend ratios of woody structures. *J Exp Bot.* Aug 1;46:981–985.

Wainwright SA, WDB, Currey JD, Gosline JM. 1982. *Mechanical design in organisms.* New York (NY): Princeton University Press.

## Appendix

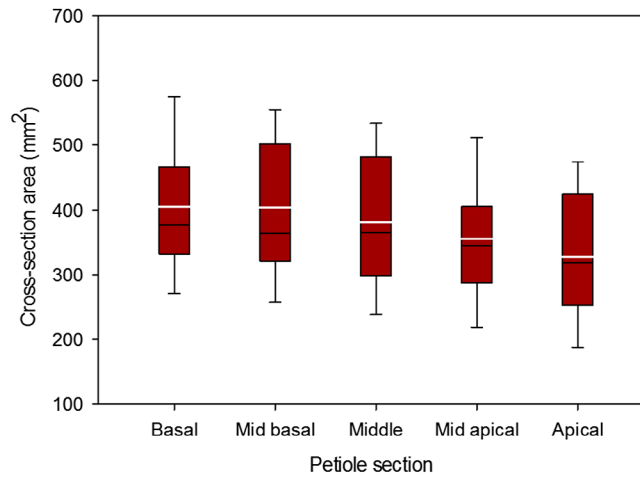


**Figure A1.** Cross-sectional area of the rhubarb petioles used for flexural testing.  
Note: White line at the middle is the mean cross-sectional area.

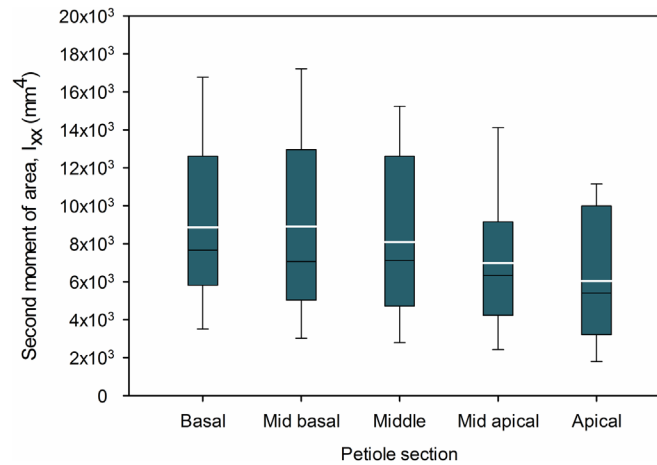


**Figure A2.** Second moment of area  $I_{xx}$  of the rhubarb petioles used for flexural testing.  
Note: White line at the middle is the mean second moment of area.

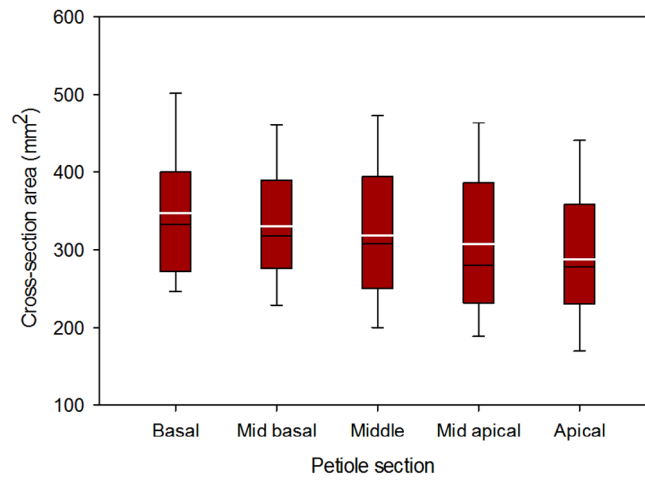


**Figure A3.** Cross-sectional area of the rhabarb petioles used for torsion testing.  
Note: White line at the middle is the mean cross-sectional area.

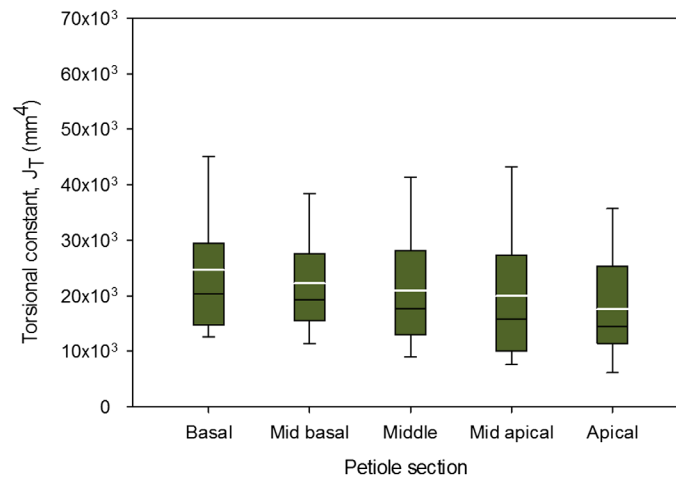


**Figure A4.** Torsion constant  $J_T$  of the rhabarb petioles used for torsion testing.  
Note: White line at the middle is the mean torsional constant.

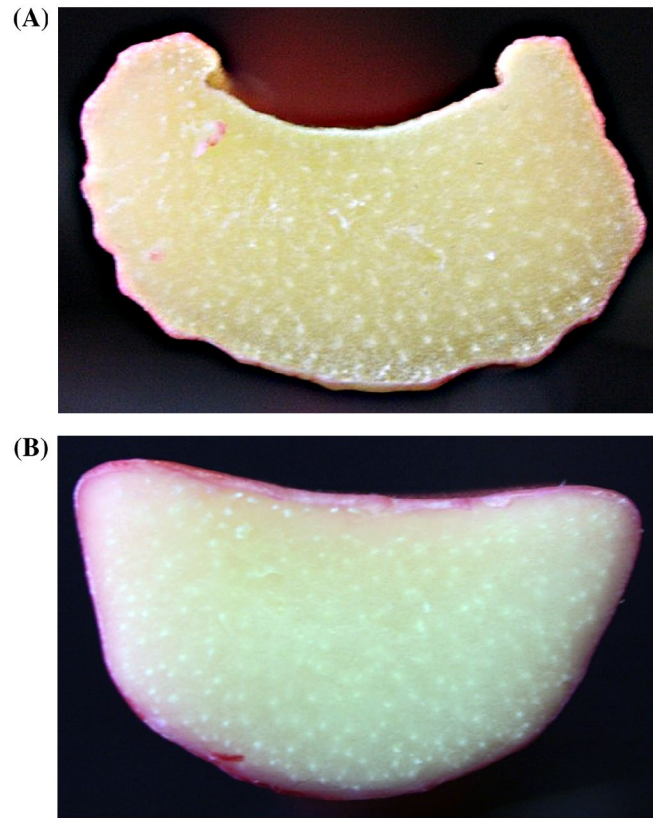


**Figure A5.** Images of typical (A) basal and (B) apical sections.